

Unleashing the Power of Undifferentiated Induced Pluripotent Stem Cell Bioprinting: Current Progress and Future Prospects

Boyoung Kim¹, Jiyeon Kim¹, Soah Lee^{1,2}

¹Department of Biopharmaceutical Convergence, Sungkyunkwan University, Suwon, Korea

²School of Pharmacy, Sungkyunkwan University, Suwon, Korea

Induced pluripotent stem cell (iPSC) technology has revolutionized various fields, including stem cell research, disease modeling, and regenerative medicine. The evolution of iPSC-based models has transitioned from conventional two-dimensional systems to more physiologically relevant three-dimensional (3D) models such as spheroids and organoids. Nonetheless, there still remain challenges including limitations in creating complex 3D tissue geometry and structures, the emergence of necrotic core in existing 3D models, and limited scalability and reproducibility. 3D bioprinting has emerged as a revolutionary technology that can facilitate the development of complex 3D tissues and organs with high scalability and reproducibility. This innovative approach has the potential to effectively bridge the gap between conventional iPSC models and complex 3D tissues *in vivo*. This review focuses on current trends and advancements in the bioprinting of iPSCs. Specifically, it covers the fundamental concepts and techniques of bioprinting and bioink design, reviews recent progress in iPSC bioprinting research with a specific focus on bioprinting undifferentiated iPSCs, and concludes by discussing existing limitations and future prospects.

Keywords: Induced pluripotent stem cells, 3D bioprinting, Tissue engineering

Introduction

Induced pluripotent stem cell (iPSC) technology has sparked a revolutionary transformation across the fields of stem cell research, developmental biology, disease modeling, and personalized medicine. iPSCs can be generated through the reprogramming of somatic cells, often achieved by overexpressing four transcription factors (i.e. Oct4, Sox2, Klf4, c-Myc) that orchestrate a pluripotency auto-reg-

ulatory circuit (1, 2). While bypassing ethical concerns associated with embryonic stem cells, iPSCs share attributes similar to embryonic stem cells, exhibiting an indefinite self-renewal capacity and remarkable potential to differentiate into the three germ layers. This facilitates studies on human development, patient-specific disease modeling, and drug testing without ethical concerns. Additionally, iPSCs represent a promising cell source for regenerative medicine as they can be used to improve the function of damaged tissues without eliciting an immune response.

To fully harness the capability of iPSCs, development of *in vitro* culture models that can support the maintenance of pluripotency of iPSCs is of great importance. Over the decades, iPSC culture condition has evolved from two-dimensional (2D) models using poorly defined, animal-derived products to the human-derived, fully defined models, to more physiologically relevant three-dimensional (3D) models (Fig. 1, Table 1) (3-7). In the beginning, iPSCs were maintained in animal-derived serum containing media on either animal-derived feeder cell layer or animal-derived extracellular matrix (ECM) coating materials

Received: September 3, 2023, Revised: November 21, 2023,

Accepted: November 21, 2023, Published online: January 2, 2024

Correspondence to **Soah Lee**

Laboratory of Tissue Engineering, School of Pharmacy, Sungkyunkwan University, 2066 Seobu-ro, Jangan-gu, Suwon 16419, Korea
E-mail: soahlee@skku.edu

© This is an open-access article distributed under the terms of the Creative Commons Attribution Non-Commercial License (<http://creativecommons.org/licenses/by-nc/4.0/>), which permits unrestricted non-commercial use, distribution, and reproduction in any medium, provided the original work is properly cited.

Copyright © 2024 by the Korean Society for Stem Cell Research

such as MatrigelTM (1, 8-10). Then, these animal derived products were replaced by human-derived products, which was still poorly defined (11-13). Further studies identified fully defined conditions, composed of soluble factors such as basic fibroblast growth factor (bFGF) and transforming growth factor- β (TGF- β), in combination with ECM proteins such as collagen IV, fibronectin, laminin, and vitronectin, for maintaining pluripotency and genomic stability of iPSCs (14-21). Advantages of utilizing fully defined 2D culture condition include (1) high reproducibility, (2) ease of high throughput analysis, and (3) relatively low variability (Fig. 1A). However, 2D culture models do not fully recapitulate 3D microenvironment, which hampers studying more physiologically relevant cell-microenvironment interactions. In addition, there is a limitation in scaling-up.

Recent studies demonstrated that 3D iPSC culture methods of forming spherical aggregates of iPSCs or spheroids for suspension culture can successfully support the maintenance of iPSC pluripotency and long-term propagation (22, 23). These iPSC spheroids can be further directed to

differentiate into multiple lineages such as brain (24, 25) and heart (26, 27), and can self-organize into organ-mimicking 3D structures, termed as organoids (Fig. 1B). These 3D iPSC culture systems reflect cell-cell and cell-ECM interactions more effectively. In addition, the system enables more scalable culture comparable to their 2D adherent counterparts. However, the current 3D iPSC culture systems often have simple geometry such as sphere, limiting construction of complex tissue structure. When grown beyond diffusion limit (~ 200 to $300 \mu\text{m}$), 3D iPSC spheroids/organoids develop a necrotic core, thereby restricting their use in long-term studies. 3D iPSC spheroids/organoids are often generated manually and thus can be a labor-intensive process with high batch variability, which limits the scalability and reproducibility.

3D bioprinting is an advanced biotechnology that involves layer-by-layer deposition of biological materials, such as cells, growth factors, and biomaterials, to construct complex 3D tissue structures. The application of 3D bioprinting to iPSCs or iPSC-derived cells can address the limitations of current 2D and 3D iPSC culture systems. Compared to monolayer 2D cultures or simple spherical 3D culture systems, 3D bioprinted iPSCs can be fabricated into complex tissue structures that mimic the architecture and functionality of native tissue at both macro- and micro-levels (Fig. 1C). Moreover, the 3D microenvironment of bioprinted iPSCs can be finely tuned for their specific applications using bioinks. Additionally, the precise and rapid control offered by 3D bioprinting enables high scalability and reproducibility.

In this review, we will discuss the latest advances in iPSC bioprinting, with a specific focus on the research progress on undifferentiated iPSC bioprinting. First, we review the concepts and techniques of 3D bioprinting, followed by the basic principles of design strategy of bioink. We then review and summarize the research advancement of 3D bioprinting especially using undifferentiated iPSCs. Finally, the current limitations and future prospects of bioprinting undifferentiated iPSCs will be discussed.

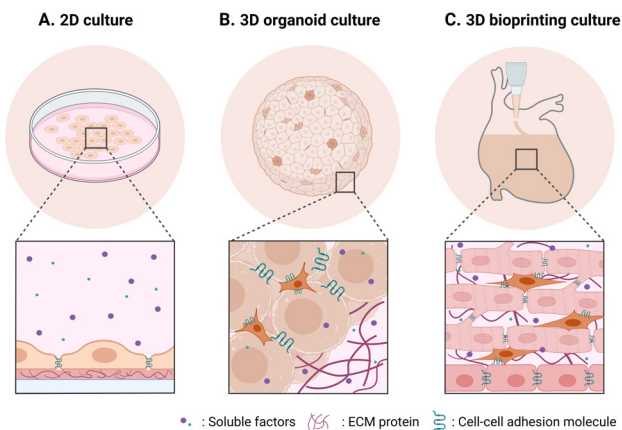


Fig. 1. Sequential evolution of induced pluripotent stem cell (iPSC)-based *in vitro* models depicting transition from 2D culture to 3D organoids, and further to 3D bioprinting. Schematics of 2D iPSC culture model (A), 3D organoid culture model (B), and 3D bioprinting culture model (C). Created with BioRender.com. ECM: extracellular matrix.

Table 1. A summary of characteristics of 2D and 3D culture models

	2D (mono-layer)	3D organoid	3D bioprinting	Reference
Mimicry of native tissue structure	Low	Intermediate	High	(3)
Maturity	Low	Intermediate	High	(4)
Cell-ECM interaction	2D	3D	Controlled 3D	(5)
Cell-cell interaction	2D	3D	Controlled 3D	(6)
Throughput	$\sim 10^2$	$\sim 10^2$	$> 10^3$	(7)

ECM: extracellular matrix.

3D Bioprinting

3D bioprinting is a cutting-edge approach to fabricating biological tissues and organs by precisely depositing cell-laden materials layer by layer, following a computer-designed blueprint. Unlike traditional 3D printing that uses various materials like plastics or metals as an ink, 3D bioprinting uses the “bio-ink” composed of living cells, bio-materials, and other biologically active compounds such as growth factors. 3D bioprinting process involves several key steps: (1) creation of digital 3D model of the desired tissue or organ based on medical images or user-defined models; (2) engineering of bioink mimicking the cellular microenvironment in the tissue of the interest; (3) bioprinting; and (4) post-printing processes such as crosslinking and maturation.

There are three representative 3D bioprinting techniques, namely inkjet-based, extrusion-based, and laser-assisted bioprinting (Fig. 2, Table 2) (28-40). These three 3D bioprinting techniques have been utilized for studies of 3D iPSC bioprinting.

Inkjet-based bioprinting

Similar to the function of a regular inkjet printer, inkjet-based bioprinting employs a print head to eject picoliter-sized droplets of bioink onto a substrate in a specific pattern at a rapid printing speed (up to 10,000 droplets per second) (41). Inkjet bioprinting is recognized for its high resolution ($50\sim 300\ \mu\text{m}$) and speed (28), making it suitable for creating intricate structures. However, it has limitations in handling viscous or dense bioinks, thereby restricting the use of materials within a narrow viscosity

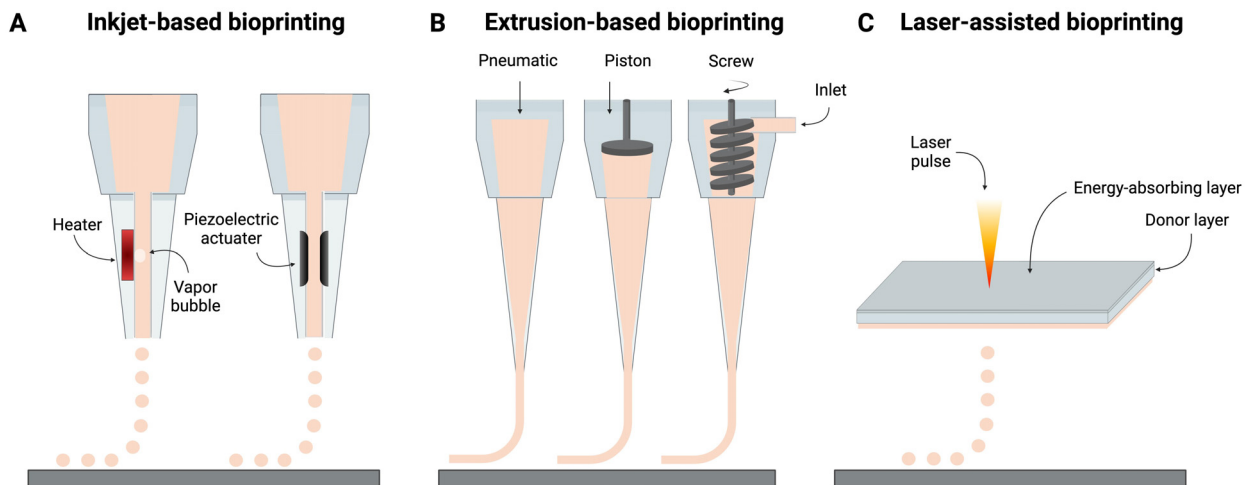


Fig. 2. Three major 3D bioprinting techniques used for induced pluripotent stem cell bioprinting. (A) Inkjet-based bioprinting, (B) extrusion-based bioprinting, and (C) laser-assisted bioprinting. Created with BioRender.com.

Table 2. A summary of bioprinting techniques used for induced pluripotent stem cell bioprinting

	Inkjet-based bioprinting	Extrusion-based bioprinting	Laser-assisted bioprinting	Reference
Printing process	Drop by drop	Line by line	Dot by dot	(28-40)
Print speed	Fast (1~10,000 droplets/s)	Slow (10~50 $\mu\text{m/s}$)	Fast (200~1,600 mm/s)	
Fabrication resolution	Relatively high (50~300 μm)	Relatively low (~200 μm)	High (>0.5~20 μm)	
Bioink preparation time	Short	Short	Long	
Cell viability	High (>85%)	Potential reduction due to pressure and shear stress	High cell viability (>95%)	
Cell density	Low (<10 ⁶ cells/ml)	High (up to 10 ⁸ cells/ml)	High (up to 10 ⁸ cells/ml)	
Throughput	High	Medium	Low-medium	
Scalability	Low	High	Low	
Bioink viscosity	3.5~12 mPa/s	30~6×10 ⁷ mPa/s	1~300 mPa/s	
Cost	Low	Medium	High	

range (3.5~12 mPa/s) and relatively low cell density ($<10^6$ cells/ml) (29, 30, 41, 42).

Extrusion-based bioprinting

In extrusion-based bioprinting, a bioink is extruded through a nozzle or syringe via pneumatic or mechanical pressure. Extrusion bioprinting presents several advantages over other printing techniques. It can handle a wide range of bioink viscosities ($30\sim6\times10^7$ mPa/s) (29) and high cell density ($>10^8$ cells/ml) (28), making it versatile for printing various tissue types. In addition, it has been demonstrated for producing human-scale large constructs (43) or large batches of tissues (44), demonstrating its high scalability. Furthermore, extrusion bioprinter is relatively cost-effective and ease of use, making it accessible to researchers (31). There are several limitations associated with extrusion bioprinting. Given the cells in bioink are subject to mechanical stress during extrusion process, cell viability and functionality may be compromised. Bioink should be carefully designed to minimize the mechanical stresses. Also, extrusion printing may have limitations in achieving high-resolution features due to the nozzle size and viscosity of bioinks. Nozzle clogging with viscous ink can also be an issue (32).

Laser-assisted bioprinting

Laser-assisted bioprinting is a sophisticated technique that employs lasers to precisely deposit cells and biomaterials in a controlled and non-contact manner. This technique utilizes the composite slide composed of an energy-absorbing layer, a donor layer, and a bioink layer containing cells and biomaterials. A pulsed laser is used to generate a focused energy pulse that creates a rapid localized pressure increase in a donor layer, leading to expelling micro-sized bioink droplets onto a substrate to form a desired pattern (45). Laser-assisted bioprinting offers several advantages including high precision ($>0.5\sim20\ \mu\text{m}$) (29, 46), non-contact printing, minimal damages from thermal and mechanical stimuli, which together reduces the risk of cell damage and nozzle clogging and enables printing of intricate tissue structures (28, 29). However, it comes with a set of challenges such as the complexity and high cost associated with the laser system and the potential need for specific laser-absorbing materials for different bioinks (29).

Each of these bioprinting techniques has its own advantages and limitations. The choice of a bioprinting technique should consider factors such as the desired tissue type and structure, and the required resolution. Depending on the selected bioprinting approach, the optimization of bioink is necessary for maximizing the potential of bioprint-

ing and creating intricate and functional tissues.

Bioink

As a key technology in 3D bioprinting, bioink is responsible for carrying and supporting encapsulated cells throughout the printing process with the ultimate goal of creating functional tissues or organs. Based on the principles of tissue engineering, bioinks are carefully formulated to contain (1) the cell types found in the target tissue; (2) biomaterials that support the viability of encapsulated cells during printing process and provide instructive, biomechanical and biochemical cues for tissue formation; and (3) bioactive factors that can guide the behaviors of encapsulated cells for functional tissue formation (Fig. 3).

Selection of cells

Selecting the right cell types in bioink is critical for achieving the desired functions of the resulting bioprinted tissues. Tissues are composed of diverse types of cells, each with unique and specialized functions. For example, in cardiac muscle tissues, cardiomyocytes are the main players responsible for contraction-relaxation function of the tissue. Other cell types, such as cardiac fibroblasts, also play an important role in maintaining the structural integrity and overall function of the cardiac muscle. One strategy is to formulate a single bioink using either a single cell type that is responsible for major tissue function (47) or a mixture of multiple cell types (48). Alternative strategy is to formulate multiple separate bioinks, each containing one cell type to achieve cell-specific distribution in the tissue (49, 50). Progenitor cells or stem cells can be used as a cell source in bioink, where they can differentiate into the

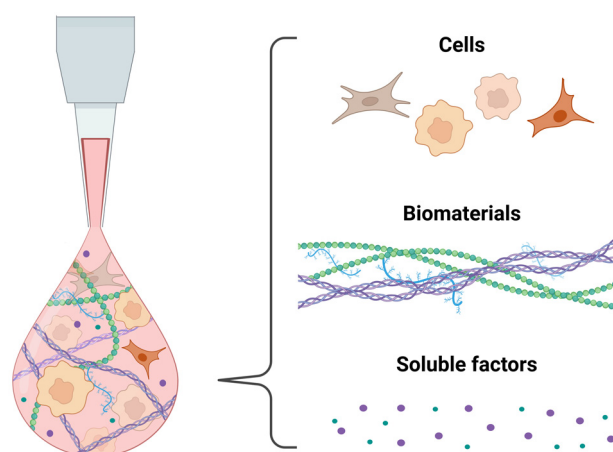


Fig. 3. Representation of bioink components used in 3D bioprinting. Created with BioRender.com.

cell types needed for creating functional tissues, with appropriate differentiation signals provided in the bioink. Multipotent stem cells such as mesenchymal stem cells or adipose-derived stem cells, as well as pluripotent stem cell-derived cells, have been widely used for 3D bioprinting (51-53). Utilizing stem cells in bioink offers several advantages over using fully differentiated cells for bioprinting. These advantages include the ability to recapitulate complex cellular diversity due to the differentiation potential of stem cells, along with achieving a more physiologically relevant cellular arrangement due to their capacity for self-organization.

Selection of biomaterials

Hydrogels are most widely used biomaterials for 3D bioink. Hydrogels are a 3D network of hydrophilic polymers that can retain water similar to body water content (~80% to 90%) with high structural integrity and biocompatibility. Hydrogels can provide and/or be easily engineered to provide biomimetic cues present in the native cellular microenvironment so that cells can grow, differentiate, and develop into functional tissues *in vitro*. Hydrogels can be categorized into two types based on their origin: (1) natural polymer-based hydrogels and (2) synthetic polymer-based hydrogels.

Natural polymer-based hydrogels are derived from naturally occurring polymers found in living organisms. Widely used natural polymers in bioink include collagen (54-56), alginate (57-59), and basement membrane proteins such as Matrigel™ (60-62). These hydrogels offer advantages such as biocompatibility, bioactivity, and biodegradability. However, their mechanical properties are often suboptimal and the tunability is limited.

Synthetic polymer-based hydrogels are created by chemically synthesized polymers and thus offer more precise control over hydrogel properties such as mechanical strength and degradation rate. Commonly used synthetic polymer-based hydrogels include polyethylene glycol (63-65) and poly(caprolactone) (66, 67). While these synthetic polymer-based hydrogels can be tailored to match the required characteristics of specific tissues and applications, they often lack bioactivity. To address the limitations, researchers have engineered the composite hydrogels by combining natural and synthetic polymers. Examples include gelatin-alginate (68-70), carboxymethyl chitosan (70, 71), and hydroxypropyl chitin (72). Researchers continue to explore novel design strategies to create hydrogels that more closely mimic the native ECM and promote tissue formation.

Selection of bioactive factors

The third component of bioink is bioactive soluble factors. Bioactive soluble factors include growth factors, cytokines, and other signaling molecules that regulate cell behaviors such as proliferation and differentiation. The goal of incorporating these factors in bioink is to create a microenvironment within the printed construct that supports cell viability, proliferation, and differentiation for tissue formation and maturation. Therefore, bioactive soluble factors need to be carefully selected based on the microenvironment of the target tissue.

Bioink design criteria

To ensure the success of the bioprinting process and the viability and functionality of the printed constructs, several design criteria of bioinks should be considered. First, bioinks must be biocompatible to ensure the viability and functionality of encapsulated cells. The components of bioink and their degraded parts should not induce toxicity or inflammation. Bioinks should also have appropriate rheological properties to ensure smooth flow of the ink during printing followed by maintenance of their shape after deposition. Printability of bioinks is influenced by the viscosity, shear-thinning property, and other mechanical properties of the bioink. Furthermore, biomimicry of bioinks is an important design criterion. Cell behaviors are well known to be guided by biomechanical and biochemical properties of the target tissue (73-76). Therefore, it is crucial to match the biomechanical properties of bioink to those of the target tissue, and to mimic the biochemical properties of bioink by incorporating relevant ECM proteins and soluble factors. Lastly, biodegradability of bioink is essential to allow encapsulated cells to form intercellular connection and remodel their surrounding environment with newly produced ECM. In sum, bioink design is a critical aspect of bioprinting to produce viable and functional bioprinted tissues for various applications.

IPSC-Based Bioprinting

Current iPSC-based bioprinting studies utilize two main strategies: (1) pre-differentiated iPSC bioprinting and (2) undifferentiated iPSC bioprinting. In the case of pre-differentiated iPSC bioprinting, iPSCs are initially differentiated into specific cell types in a conventional 2D culture condition. Subsequently, these cells are encapsulated in cell-specific bioink for 3D bioprinting (Fig. 4A). On the other hand, the approach of undifferentiated iPSC-based bioprinting, also known as post-differentiation iPSC-based bioprinting, involves the direct encapsulation and 3D bio-

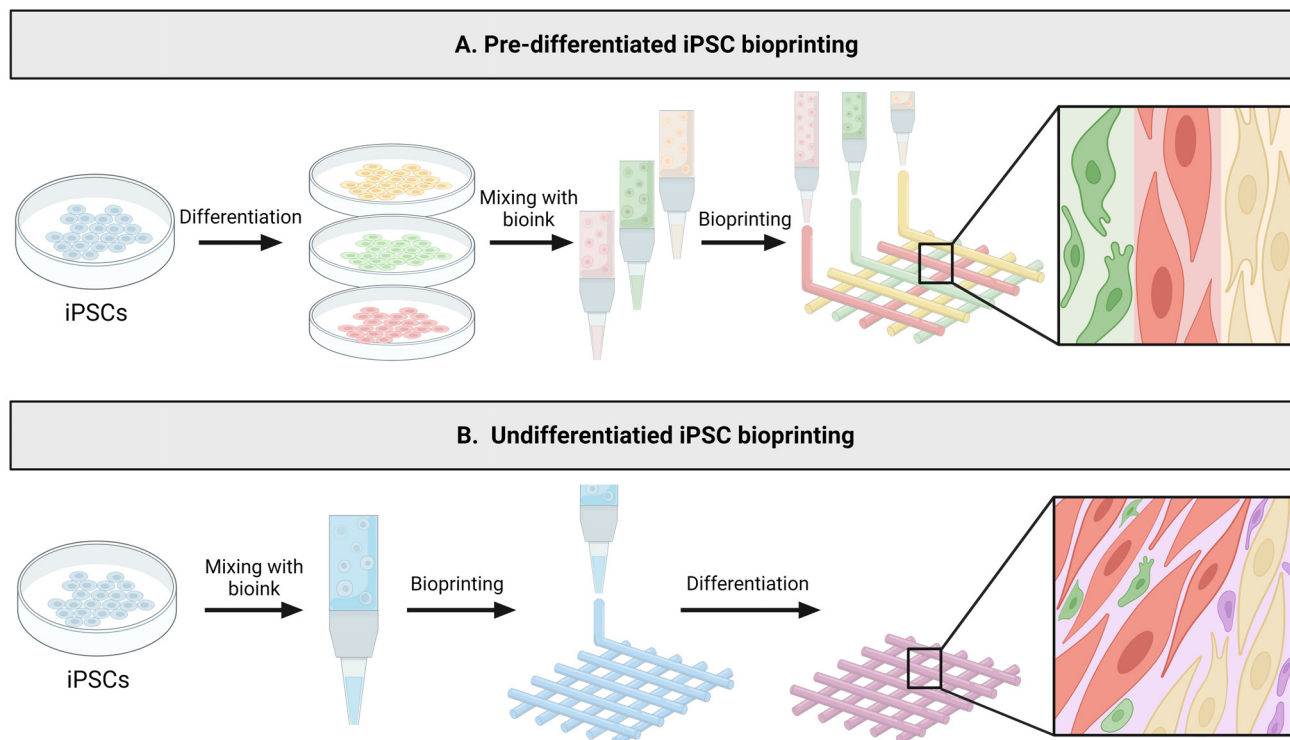


Fig. 4. Induced pluripotent stem cell (iPSC)-based bioprinting strategies. Processes for pre-differentiated iPSC bioprinting (A) and undifferentiated iPSC bioprinting (B). Created with BioRender.com.

printing of undifferentiated iPSCs. Following printing, these iPSCs are directed to differentiate into specific lineage within the bioprinted tissue construct (Fig. 4B). The selection and application of the iPSC-based bioprinting strategies should consider the respective advantages and disadvantages associated with each method.

Pre-differentiated iPSC bioprinting

Previous studies have extensively utilized pre-differentiated iPSC bioprinting to fabricate a range of tissues, including cartilage, heart, nerve, liver, and skin. This topic has been thoroughly reviewed in numerous review articles, and thus it is not within the scope of this review (please refer to (77)).

Utilizing pre-differentiated iPSCs provides several advantages. First, it provides better control over bioink formulation due to a more controlled differentiation of iPSCs in a 2D setting. Additionally, the pre-differentiated iPSCs can be encapsulated in biomaterials customized to guide specific cellular behaviors in a cell-specific manner. By utilizing multiple cell-type-specific bioinks, it is possible to recapitulate the diversity and distribution of cells present in tissue through spatial patterning of various cell types. For example, Noor et al. (50) used two cell-specific bioinks, namely a cardiomyocyte-specific, and endothelial cell-spe-

cific bioinks to create structurally complex and functional cardiac tissues. However, pre-differentiated iPSC bioprinting has its disadvantages. The resolution of current bioprinting technology limits the recreation of micro-structures present in tissues. Also, cell-cell integration is restricted, particularly between cells in different bioinks (49, 78-80).

Undifferentiated iPSC bioprinting

Compared to pre-differentiated iPSC bioprinting, the bioprinting of undifferentiated iPSCs has received relatively less attention. One of the advantages of undifferentiated iPSC bioprinting is the versatility of the printed tissue constructs as they can subsequently undergo differentiation into various tissues. In addition, since iPSCs, during differentiation, give rise to diverse cell types found in tissues and these cells can self-organize, post-differentiation of the bioprinted iPSC constructs closely emulate the process of organoid formation, which can lead to better recapitulating the native tissue structure and function. Moreover, thanks to their remarkable proliferative capacity, the formation of stable and well-connected tissue structures can be more readily achievable (81). In the following section, we will summarize the research progress on the bioink laden with undifferentiated iPSCs.

Bioink development for undifferentiated iPSC bioprinting

Previous studies have reported the development of undifferentiated iPSC-laden bioink that supports high viability post-printing and maintains pluripotency (Table 3) (49, 59, 72, 81-85). Earlier research adopted two distinct strategies for creating bioinks containing undifferentiated iPSCs: one without scaffolding materials and the other incorporating scaffolding materials. The use of undifferentiated iPSC-laden bioink without scaffolding materials facilitates cellular proliferation and the secretion of ECMs, resulting in the formation of tissue structures resembling the process of organoid development. Due to its simplicity, this strategy was employed to generate a high-throughput array of spheroids or organoids (82). Nonetheless, bioprinting iPSCs without scaffolding materials poses limitations on fabricating intricate 3D structures. Hence, the incorporation of scaffolding materials in bioink is imperative for achieving more complex 3D structure.

In order to bioprint complex 3D structures using undifferentiated iPSCs, researchers have investigated the utilization of diverse combinations of biomaterials and bioactive factors to formulate undifferentiated iPSC-laden bioinks. One of the commonly used biomaterials is alginate (49, 83, 84). Alginate is a polysaccharide extracted from brown algae, that has been widely used as a tissue engineering scaffold due to its biocompatibility, non-immunogenicity, low toxicity, and hydrophilicity (86). Alginate, a negatively charged polymer, can rapidly be crosslinked under the presence of calcium ions and its viscosity can be easily controlled, which makes it an attractive material for bioink. Since alginate lacks bioactivity, it is essential to add ECM proteins and bioactive factors to support the viability and maintenance of pluripotency in encapsulated iPSCs. Particularly, a mixture of basement membrane proteins derived from mouse sarcoma tissue, such as MatrigelTM or GeltrexTM, has been used to enhance the bioactivity (72, 82, 84, 85). It was reported that increasing MatrigelTM concentration leads to an increase in survival and aggregation of the iPSCs (72). Employing these bioinks, previous studies have demonstrated that the bioprinted iPSCs can retain their pluripotency, along with the capability to undergo spontaneous differentiation into the three germ layers and even be guided towards cardiomyocyte differentiation. (82, 85).

Since MatrigelTM or GeltrexTM originates from animal sarcoma tissues, and their components are poorly defined, efforts have been made to develop novel bioinks with more defined bioactive components. For instance, when alginate-based bioinks were supplemented with chitosan or fibrinogen, the encapsulated undifferentiated iPSCs showed

pluripotency marker expression (OCT4, SOX2, NANOG, SSEA4, TRA-1-60), proliferation, and differentiation into three germ layers (49, 83). Nonetheless, these proteins are not naturally present during embryo development. Additional research is necessary to determine whether recapitulating the microenvironment of epiblasts can further enhance the self-renewal and differentiation capacity of the bioprinted iPSCs.

Precisely guiding the fate of iPSCs into tissues of interest is another important aspect to consider when designing an iPSC-laden bioink. It is well-known that iPSC differentiation can be efficiently guided by mimicking the native cellular microenvironment of the desired tissue (87). To design biomimetic bioinks, the microenvironment of the targeted tissue can be recapitulated by including combinations of ECM components and growth factors abundantly found in the tissue, or using decellularized ECM derived from the tissue (Table 4) (88-101). There are only a few studies on an undifferentiated iPSC-laden bioink that is inductive to differentiation by mimicking the microenvironment of the target tissue. For example, Kupfer et al. (81) demonstrated the differentiation of bioprinted iPSCs into cardiomyocytes and the formation of perfusable two-chambered hearts by developing a novel bioink composed of defined components—collagen methacrylate, laminin-111, and fibronectin—that are known to promote cardiac cell differentiation. Similarly, Nguyen et al. (84) employed a bioink incorporating hyaluronic acid, a key component of the chondrocyte microenvironment, to promote the differentiation of chondrogenic lineages after undifferentiated iPSC bioprinting. In summary, tissue-mimetic bioinks designed for bioprinting undifferentiated iPSCs have been demonstrated to be effective to support viability, preserve pluripotency, and enable both spontaneous and directed differentiations.

Challenges and Future Prospects of Undifferentiated iPSC Bioprinting

Previous studies on undifferentiated iPSC bioprinting have demonstrated high viability, pluripotency retention, and differentiation potential post-printing. Despite these advancements, there are still several limitations that need to be addressed for the broader application of undifferentiated iPSC bioprinting.

First, most previous studies demonstrated bioprinting undifferentiated iPSCs in simple tissue structures such as droplet (82, 85) or grid structures (49, 72, 83, 84). Future studies should explore printing more sophisticated structures that are physiologically relevant. Another bottleneck of undifferentiated iPSC bioprinting technology is poor in

Table 3. A summary of undifferentiated induced pluripotent stem cell bioprinting

Printing technique	Nozzle diameter (μm)	Bioink	Crosslinker	Construct design	Cell concentration (cells/ml)	Characterization	Reference
Extrusion	101.6	1.5% w/v alginate	600 mM CaCl_2	Ring structure	1×10^6	Pluripotency: flow cytometry (OCT3/4, SSEA4)	(59)
	40	Geltrex™	-	100 nl droplet	4.5×10^6	Pluripotency: immunostaining (TRA-1-81), qRT-PCR (NANOG) Spontaneous differentiation: qRT-PCR (PAX3, HAND1, SOX17)	(82)
	200	5% w/v alginate, 5% w/v carboxymethyl-chitosan, 1.5% w/v agarose	2% CaCl_2 for 10 min	Grid structure	8×10^7	Proliferation: PrestoBlue assay Pluripotency: flow cytometry (OCT4, SOX2, TRA-1-60, SSEA4), immunostaining (OCT4, SOX2, SSEA4, TRA-1-60) Spontaneous differentiation: qRT-PCR (H19, PDX1, HAND1, IGF2, NES, TUBB3)	(83)
	300	NFC alginate (60 : 40), NFC with hyaluronic acid	100 mM CaCl_2 , 0.001% H_2O_2	Grid structure	2×10^7	Directed neural differentiation: immunostaining (PAX6, NES, MAP2, GFAP, TUBB3, SYP, GABA), qRT-PCR (NES, TUBB3, GFAP, GABA, NKX2-1, PET1, OLIG2) Pluripotency: immunostaining (OCT4) Spontaneous differentiation: qRT-PCR (SOX9, ACAN, Coll 2A1) Directed chondrogenic differentiation: Alcian blue-van Gieson staining (GAG), Safranin-O staining, immunostaining (Collagen type II)	(84)
	260	2% w/v hydroxypropyl chitin (HPCH), 0% ~ 30% Matrigel™	Temperature 37°C	Grid structure	1×10^6	Proliferation: Cell Counting Kit-8 assay	(72)
	260	4% w/w alginate, 1% w/w polyethylene glycol fibrinogen	0.3 M CaCl_2 , 365 nm UV for 5 min	Grid structure	8×10^6	Pluripotency: AP staining, immunostaining (OCT4, SSEA4), flow cytometry (OCT4, SSEA4), qRT-PCR (OCT4, NANOG) Proliferation: immunostaining (Ki67) Pluripotency: qRT-PCR (OCT4, SOX2, NANOG), immunostaining (OCT4)	(49)
	210	10% gelatin methacrylate, fibronectin, laminin-111, collagen methacrylate	405 nm flashlight for 20 sec	Human chambered muscle pumps	1.5×10^7	Proliferation: immunostaining (Ki67) Directed cardiac differentiation: immunostaining (cTnT, TUNEL, α SMA, CD31, CX43, Bin1, RYR2, SERCA2, α -actin, cTnI)	(81)
Laser	N/A	1 wt% hyaluronic acid, Matrigel™	N/A	0.01 ~ 1 nl droplets	3.3×10^7	Proliferation: LDH activity assay, Tripzan blue staining, MTT assay, immunostaining (Ki67) Pluripotency: ALP assay, immunostaining (OCT3/4, NANOG, ALP, SSEA4) Spontaneous differentiation: immunostaining (β III Tubulin, Cytokeratin 8, AFP, SMA, von Willebrand factor, α -actinin) Directed cardiac differentiation: immunostaining (Brachyury, cTnT, NKX2.5, α -actinin)	(85)

N/A: not available, NFC: nanofibrillated cellulose, UV: ultraviolet.

Table 4. Biomechanical and biochemical characterization of tissues for induced pluripotent stem cell bioink design

	Biochemical		Biomechanical	Reference
	Extracellular matrix (ECM) component	Soluble factor	Stiffness (elastic modulus) (kPa) (88, 89)	
Brain	Proteoglycans (aggrecan, brevican, versican, neurocan, phosphacan, syndecan, glypican, agrin) Glycoproteins (link protein, tenascin-R, collagens, fibronectin, laminin, nidogen) Glycosaminoglycan (hyaluronic acid) Glycoproteins (collagen, laminin, fibronectin, tenascin, nidogen)	Glia-derived neurotrophic factor (GDNF) Brain-derived neurotrophic factor (BDNF) Nerve growth factor (NGF) Neurotrophin-3 (NT-3)	0.5~3	(90-92)
Liver	Glycoproteins (collagen, laminin, fibronectin, tenascin, nidogen) Proteoglycans (heparan, dermatan, chondroitin sulphate, perlecan, biglycan, decorin) Glycosaminoglycan (hyaluronic acid)	PDGF FGF VEGF Endothelin-1 (ET-1) EGF Insulin growth factor Transforming growth factor beta (TGF- β)	5~10	(93, 94)
Lung	Glycoproteins (collagen, fibronectin, laminin, elastin) Proteoglycans (chondroitin sulphate) Glycosaminoglycan	FGF Bone morphogenetic protein 4 (BMP4) Hepatocyte growth factor (HGF)	0.5~15	(95, 96)
Heart	Glycoproteins (collagen, laminin, fibronectin, elastin) Proteoglycans (chondroitin sulphate, versican) Glycosaminoglycan	FGF VEGF EGF Tissue growth factors (TGFs)	10~15	(97, 98)
Skin	Glycoproteins (collagen, elastin, fibronectin, laminin) Proteoglycans (heparan sulfate, chondroitin sulfate, keratan sulfate) Glycosaminoglycans (hyaluronic acid, chondroitin, dermatan, heparin), keratin	EGF Basic fibroblast growth factor (bFGF) VEGF PDGF Keratinocyte growth factor (KGF)	60~850	(99, 100)
Bone	Glycoprotein (collagen type-1) Carbonated apatite	VEGF Bone morphogenetic proteins (BMP2, BMP7)	15,000~20,000	(101)

PDGF: platelet-derived growth factor, FGF: fibroblast growth factor, VEGF: vascular endothelial growth factor, EGF: epidermal growth factor.

tercellular integration post-printing. Although iPSCs present remarkable proliferative capacity, current bioinks reported seem insufficient to support proliferation, migration, and tissue formation. This can be overcome by several strategies such as using cell aggregates rather than single cells (102, 103) and incorporating inductive ECM proteins and/or bioactive molecules that can promote proliferation and migration. Furthermore, previous studies have only validated three germ layer specification and directed differentiation towards only one or two selected cell types such as neuron, chondrocyte, or cardiomyocytes (81, 83-85). Since iPSCs possess broad differentiation potentials, it would be interesting to explore the versatility of the undifferentiated iPSC-laden bioink. For example, it is worth investigating whether bioprinted undifferentiated iPSCs using one type of bioink can be further differentiated into diverse cell types post-printing. Finally, for producing 3D complex and thick tissues, the creation of intricate vascular network structures is imperative to prevent cellular necrosis within the inner regions of the bioprinted tissues.

Undifferentiated iPSC bioprinting holds promising future prospects for advancing various research fields, including tissue engineering, developmental biology, disease modeling, and drug screening. Specifically, undifferentiated iPSC bioprinting has the potential to revolutionize personalized medicine by enabling the construction of patient-specific tissues that mimic the intricate geometry and structures of native tissues and organs. Integrating undifferentiated iPSC bioprinting with microfluidic systems could lead to the development of novel “organ-on-a-chip” platforms, offering a more precise representation of human physiological system for developmental studies and disease modeling. The capability to bioprint arrays of undifferentiated iPSCs could enhance scalability and reduce variability, and thereby facilitate high-throughput drug screening. This innovative technology offers an alternative to using model organism-based preclinical models, holding the potential to facilitate the drug development process. As such, these prospects highlight the exciting potential of undifferentiated iPSC bioprinting, which converges cutting-edge iPSC technology and 3D bioprinting techniques, accelerating both basic research and the translation of scientific discoveries into therapeutic applications.

ORCID

Boyoung Kim, <https://orcid.org/0009-0000-7250-8565>

Jiyeon Kim, <https://orcid.org/0009-0009-9174-6476>

Soah Lee, <https://orcid.org/0000-0001-7613-592X>

Funding

This research was supported by Basic Science Research Program through the National Research Foundation of Korea (NRF) funded by the Ministry of Education (MOE, 2022R1A6A1A03054419), Korean Fund for Regenerative Medicine funded by Ministry of Science and ICT, and Ministry of Health and Welfare (22A0302L1-01, Republic of Korea). The SungKyunKwan University and the BK21 FOUR (Graduate School Innovation) funded by the MOE and NRF.

Potential Conflict of Interest

There is no potential conflict of interest to declare.

Authors' Contribution

Conceptualization: BK, SL. Funding acquisition: SL. Investigation: BK, JK, SL. Visualization: BK, SL. Writing – original draft: BK, JK, SL. Writing – review and editing: BK, SL.

References

1. Takahashi K, Tanabe K, Ohnuki M, et al. Induction of pluripotent stem cells from adult human fibroblasts by defined factors. *Cell* 2007;131:861-872
2. Takahashi K, Yamanaka S. Induction of pluripotent stem cells from mouse embryonic and adult fibroblast cultures by defined factors. *Cell* 2006;126:663-676
3. Jensen C, Teng Y. Is it time to start transitioning from 2D to 3D cell culture? *Front Mol Biosci* 2020;7:33
4. Duval K, Grover H, Han LH, et al. Modeling physiological events in 2D vs. 3D cell culture. *Physiology (Bethesda)* 2017;32:266-277
5. Kim J, Koo BK, Knoblich JA. Human organoids: model systems for human biology and medicine. *Nat Rev Mol Cell Biol* 2020;21:571-584
6. Hofer M, Lutolf MP. Engineering organoids. *Nat Rev Mater* 2021;6:402-420
7. Kačarević ŽP, Rider PM, Alkildani S, et al. An introduction to 3D bioprinting: possibilities, challenges and future aspects. *Materials (Basel)* 2018;11:2199
8. Thomson JA, Itskovitz-Eldor J, Shapiro SS, et al. Embryonic stem cell lines derived from human blastocysts. *Science* 1998;282:1145-1147
9. Hoffman LM, Carpenter MK. Characterization and culture of human embryonic stem cells. *Nat Biotechnol* 2005; 23:699-708
10. Yu J, Hu K, Smuga-Otto K, et al. Human induced pluripotent stem cells free of vector and transgene sequences. *Science* 2009;324:797-801
11. Ludwig TE, Levenstein ME, Jones JM, et al. Derivation of human embryonic stem cells in defined conditions. *Nat Biotechnol* 2006;24:185-187
12. Richards M, Fong CY, Chan WK, Wong PC, Bongso A.

- Human feeders support prolonged undifferentiated growth of human inner cell masses and embryonic stem cells. *Nat Biotechnol* 2002;20:933-936
13. Richards M, Tan S, Fong CY, Biswas A, Chan WK, Bongso A. Comparative evaluation of various human feeders for prolonged undifferentiated growth of human embryonic stem cells. *Stem Cells* 2003;21:546-556
 14. Amit M, Carpenter MK, Inokuma MS, et al. Clonally derived human embryonic stem cell lines maintain pluripotency and proliferative potential for prolonged periods of culture. *Dev Biol* 2000;227:271-278
 15. Xu RH, Peck RM, Li DS, Feng X, Ludwig T, Thomson JA. Basic FGF and suppression of BMP signaling sustain undifferentiated proliferation of human ES cells. *Nat Methods* 2005;2:185-190
 16. Watanabe K, Ueno M, Kamiya D, et al. A ROCK inhibitor permits survival of dissociated human embryonic stem cells. *Nat Biotechnol* 2007;25:681-686
 17. Braam SR, Zeinstra L, Litjens S, et al. Recombinant vitronectin is a functionally defined substrate that supports human embryonic stem cell self-renewal via α 5 β 1 integrin. *Stem Cells* 2008;26:2257-2265
 18. Miyazaki T, Futaki S, Suemori H, et al. Laminin E8 fragments support efficient adhesion and expansion of dissociated human pluripotent stem cells. *Nat Commun* 2012;3:1236
 19. Rodin S, Domogatskaya A, Ström S, et al. Long-term self-renewal of human pluripotent stem cells on human recombinant laminin-511. *Nat Biotechnol* 2010;28:611-615
 20. Rodin S, Antonsson L, Hovatta O, Tryggvason K. Monolayer culturing and cloning of human pluripotent stem cells on laminin-521-based matrices under xeno-free and chemically defined conditions. *Nat Protoc* 2014;9:2354-2368
 21. Rodin S, Antonsson L, Niaudet C, et al. Clonal culturing of human embryonic stem cells on laminin-521/E-cadherin matrix in defined and xeno-free environment. *Nat Commun* 2014;5:3195
 22. Olmer R, Haase A, Merkert S, et al. Long term expansion of undifferentiated human iPS and ES cells in suspension culture using a defined medium. *Stem Cell Res* 2010;5:51-64
 23. Steiner D, Khaner H, Cohen M, et al. Derivation, propagation and controlled differentiation of human embryonic stem cells in suspension. *Nat Biotechnol* 2010;28:361-364
 24. Lancaster MA, Renner M, Martin CA, et al. Cerebral organoids model human brain development and microcephaly. *Nature* 2013;501:373-379
 25. Qian X, Nguyen HN, Song MM, et al. Brain-region-specific organoids using mini-bioreactors for modeling ZIKV exposure. *Cell* 2016;165:1238-1254
 26. Hofbauer P, Jahnel SM, Papai N, et al. Cardioids reveal self-organizing principles of human cardiogenesis. *Cell* 2021;184:3299-3317.e22
 27. Lewis-Israeli YR, Wasserman AH, Gabalski MA, et al. Self-assembling human heart organoids for the modeling of cardiac development and congenital heart disease. *Nat Commun* 2021;12:5142
 28. Murphy SV, Atala A. 3D bioprinting of tissues and organs. *Nat Biotechnol* 2014;32:773-785
 29. Arslan-Yildiz A, El Assal R, Chen P, Guven S, Inci F, Demirci U. Towards artificial tissue models: past, present, and future of 3D bioprinting. *Biofabrication* 2016;8:014103
 30. Hözl K, Lin S, Tytgat L, Van Vlierberghe S, Gu L, Ovsianikov A. Bioink properties before, during and after 3D bioprinting. *Biofabrication* 2016;8:032002
 31. Khoeni R, Nosrati H, Akbarzadeh A, et al. Natural and synthetic bioinks for 3D bioprinting. *Adv NanoBiomed Res* 2021;1:2000097
 32. Vijayavenkataraman S, Yan WC, Lu WF, Wang CH, Fuh JYH. 3D bioprinting of tissues and organs for regenerative medicine. *Adv Drug Deliv Rev* 2018;132:296-332
 33. Guillemot F, Souquet A, Catros S, et al. High-throughput laser printing of cells and biomaterials for tissue engineering. *Acta Biomater* 2010;6:2494-2500
 34. Kim JD, Choi JS, Kim BS, Chan Choi Y, Cho YW. Piezoelectric inkjet printing of polymers: stem cell patterning on polymer substrates. *Polymer* 2010;51:2147-2154
 35. Chang CC, Boland ED, Williams SK, Hoying JB. Direct-write bioprinting three-dimensional biohybrid systems for future regenerative therapies. *J Biomed Mater Res B Appl Biomater* 2011;98:160-170
 36. Koch L, Kuhn S, Sorg H, et al. Laser printing of skin cells and human stem cells. *Tissue Eng Part C Methods* 2010;16:847-854
 37. Michael S, Sorg H, Peck CT, et al. Tissue engineered skin substitutes created by laser-assisted bioprinting form skin-like structures in the dorsal skin fold chamber in mice. *PLoS One* 2013;8:e57741
 38. Norotte C, Marga FS, Niklason LE, Forgacs G. Scaffold-free vascular tissue engineering using bioprinting. *Biomaterials* 2009;30:5910-5917
 39. Smith CM, Stone AL, Parkhill RL, et al. Three-dimensional bioassembly tool for generating viable tissue-engineered constructs. *Tissue Eng* 2004;10:1566-1576
 40. Marga F, Jakob K, Khatiwala C, et al. Toward engineering functional organ modules by additive manufacturing. *Biofabrication* 2012;4:022001
 41. Li X, Liu B, Pei B, et al. Inkjet Bioprinting of Biomaterials. *Chem Rev* 2020;120:10793-10833
 42. Xu T, Jin J, Gregory C, Hickman JJ, Boland T. Inkjet printing of viable mammalian cells. *Biomaterials* 2005;26:93-99
 43. Mirdamadi E, Tashman JW, Shiwarski DJ, Palchesko RN, Feinberg AW. FRESH 3D bioprinting a full-size model of the human heart. *ACS Biomater Sci Eng* 2020;6:6453-6459
 44. Kim E, Choi S, Kang B, et al. Creation of bladder assembloids mimicking tissue regeneration and cancer. *Nature* 2020;588:664-669
 45. Guillotin B, Souquet A, Catros S, et al. Laser assisted bioprinting of engineered tissue with high cell density and microscale organization. *Biomaterials* 2010;31:7250-7256
 46. Zhu W, Ma X, Gou M, Mei D, Zhang K, Chen S. 3D printing of functional biomaterials for tissue engineering. *Curr Opin Biotechnol* 2016;40:103-112

47. Yu C, Ma X, Zhu W, et al. Scanningless and continuous 3D bioprinting of human tissues with decellularized extracellular matrix. *Biomaterials* 2019;194:1-13
48. Coffin BD, Hudson AR, Lee A, Feinberg AW. FRESH 3D bioprinting a ventricle-like cardiac construct using human stem cell-derived cardiomyocytes. *Methods Mol Biol* 2022; 2485:71-85
49. Maiullari F, Costantini M, Milan M, et al. A multi-cellular 3D bioprinting approach for vascularized heart tissue engineering based on HUVECs and iPSC-derived cardiomyocytes. *Sci Rep* 2018;8:13532
50. Noor N, Shapira A, Edri R, Gal I, Wertheim L, Dvir T. 3D printing of personalized thick and perfusable cardiac patches and hearts. *Adv Sci (Weinh)* 2019;6:1900344
51. Lawlor KT, Vanslambrouck JM, Higgins JW, et al. Cellular extrusion bioprinting improves kidney organoid reproducibility and conformation. *Nat Mater* 2021;20:260-271
52. Choi K, Park CY, Choi JS, et al. The effect of the mechanical properties of the 3D printed gelatin/hyaluronic acid scaffolds on hMSCs differentiation towards chondrogenesis. *Tissue Eng Regen Med* 2023;20:593-605
53. Narayanan LK, Huebner P, Fisher MB, Spang JT, Starly B, Shirwaiker RA. 3D-bioprinting of polylactic acid (PLA) nanofiber-alginate hydrogel bioink containing human adipose-derived stem cells. *ACS Biomater Sci Eng* 2016;2: 1732-1742
54. Osidak EO, Karalkin PA, Osidak MS, et al. Viscoll collagen solution as a novel bioink for direct 3D bioprinting. *J Mater Sci Mater Med* 2019;30:31
55. Duarte Campos DF, Rohde M, Ross M, et al. Corneal bioprinting utilizing collagen-based bioinks and primary human keratocytes. *J Biomed Mater Res A* 2019;107:1945-1953
56. Park JA, Lee HR, Park SY, Jung S. Self-organization of fibroblast-laden 3D collagen microstructures from inkjet-printed cell patterns. *Adv Biosyst* 2020;4:e1900280
57. Säljö K, Orrhult LS, Apelgren P, Markstedt K, Kölby L, Gatenholm P. Successful engraftment, vascularization, and *In vivo* survival of 3D-bioprinted human lipoaspirate-derived adipose tissue. *Bioprinting* 2020;17:e00065
58. Kim MH, Lee YW, Jung WK, Oh J, Nam SY. Enhanced rheological behaviors of alginate hydrogels with carrageenan for extrusion-based bioprinting. *J Mech Behav Biomed Mater* 2019;98:187-194
59. Faulkner-Jones A, Fyfe C, Cornelissen DJ, et al. Bioprinting of human pluripotent stem cells and their directed differentiation into hepatocyte-like cells for the generation of mini-livers in 3D. *Biofabrication* 2015;7:044102
60. Poldervaart MT, Gremmels H, van Deventer K, et al. Prolonged presence of VEGF promotes vascularization in 3D bioprinted scaffolds with defined architecture. *J Control Release* 2014;184:58-66
61. Snyder JE, Hamid Q, Wang C, et al. Bioprinting cell-laden matrigel for radioprotection study of liver by pro-drug conversion in a dual-tissue microfluidic chip. *Biofabrication* 2011;3:034112
62. Berg J, Hiller T, Kissner MS, et al. Optimization of cell-laden bioinks for 3D bioprinting and efficient infection with influenza A virus. *Sci Rep* 2018;8:13877
63. Xin S, Chimene D, Garza JE, Gaharwar AK, Alge DL. Clickable PEG hydrogel microspheres as building blocks for 3D bioprinting. *Biomater Sci* 2019;7:1179-1187
64. Skardal A, Zhang J, Prestwich GD. Bioprinting vessel-like constructs using hyaluronan hydrogels crosslinked with tetrahedral polyethylene glycol tetracrylates. *Biomaterials* 2010; 31:6173-6181
65. Dubbin K, Tabet A, Heilshorn SC. Quantitative criteria to benchmark new and existing bio-inks for cell compatibility. *Biofabrication* 2017;9:044102
66. Borkar T, Goenka V, Jaiswal AK. Application of poly- ϵ -caprolactone in extrusion-based bioprinting. *Bioprinting* 2021;21:e00111
67. Merceron TK, Burt M, Seol YJ, et al. A 3D bioprinted complex structure for engineering the muscle-tendon unit. *Biofabrication* 2015;7:035003
68. Duan B, Hockaday LA, Kang KH, Butcher JT. 3D bioprinting of heterogeneous aortic valve conduits with alginate/gelatin hydrogels. *J Biomed Mater Res A* 2013;101:1255-1264
69. Pataky K, Braschler T, Negro A, Renaud P, Lutolf MP, Brugger J. Microdrop printing of hydrogel bioinks into 3D tissue-like geometries. *Adv Mater* 2012;24:391-396
70. Huang J, Fu H, Wang Z, et al. BMSCs-laden gelatin/sodium alginate/carboxymethyl chitosan hydrogel for 3D bioprinting. *RSC Adv* 2016;6:108423-108430
71. Rajabi M, McConnell M, Cabral J, Ali MA. Chitosan hydrogels in 3D printing for biomedical applications. *Carbohydr Polym* 2021;260:117768
72. Li Y, Jiang X, Li L, et al. 3D printing human induced pluripotent stem cells with novel hydroxypropyl chitin bioink: scalable expansion and uniform aggregation. *Biofabrication* 2018;10:044101
73. Engler AJ, Sen S, Sweeney HL, Discher DE. Matrix elasticity directs stem cell lineage specification. *Cell* 2006;126: 677-689
74. Engler AJ, Carag-Krieger C, Johnson CP, et al. Embryonic cardiomyocytes beat best on a matrix with heart-like elasticity: scar-like rigidity inhibits beating. *J Cell Sci* 2008; 121(Pt 22):3794-3802
75. Lee S, Stanton AE, Tong X, Yang F. Hydrogels with enhanced protein conjugation efficiency reveal stiffness-induced YAP localization in stem cells depends on biochemical cues. *Biomaterials* 2019;202:26-34
76. Chaudhuri O, Cooper-White J, Janmey PA, Mooney DJ, Shenoy VB. Effects of extracellular matrix viscoelasticity on cellular behaviour. *Nature* 2020;584:535-546
77. Ong CS, Yesantharao P, Huang CY, et al. 3D bioprinting using stem cells. *Pediatr Res* 2018;83:223-231
78. Zhang YS, Arneri A, Bersini S, et al. Bioprinting 3D microfibrous scaffolds for engineering endothelialized myocardium and heart-on-a-chip. *Biomaterials* 2016;110:45-59
79. Billiet T, Gevaert E, De Schryver T, Cornelissen M, Dubrue P. The 3D printing of gelatin methacrylamide cell-laden tissue-engineered constructs with high cell viability.

- Biomaterials 2014;35:49-62
80. Rutz AL, Hyland KE, Jakus AE, Burghardt WR, Shah RN. A multimaterial bioink method for 3D printing tunable, cell-compatible hydrogels. *Adv Mater* 2015;27:1607-1614
 81. Kupfer ME, Lin WH, Ravikumar V, et al. In situ expansion, differentiation, and electromechanical coupling of human cardiac muscle in a 3D bioprinted, chambered organoid. *Circ Res* 2020;127:207-224
 82. Reid JA, Mollica PA, Johnson GD, Ogle RC, Bruno RD, Sachs PC. Accessible bioprinting: adaptation of a low-cost 3D-printer for precise cell placement and stem cell differentiation. *Biofabrication* 2016;8:025017
 83. Gu Q, Tomaskovic-Crook E, Wallace GG, Crook JM. 3D bioprinting human induced pluripotent stem cell constructs for in situ cell proliferation and successive multilineage differentiation. *Adv Healthc Mater* 2017;6:1700175
 84. Nguyen D, Hägg DA, Forsman A, et al. Cartilage tissue engineering by the 3D bioprinting of iPS cells in a nanocellulose/alginate bioink. *Sci Rep* 2017;7:658
 85. Koch L, Deiwick A, Franke A, et al. Laser bioprinting of human induced pluripotent stem cells—the effect of printing and biomaterials on cell survival, pluripotency, and differentiation. *Biofabrication* 2018;10:035005
 86. Axpe E, Oyen ML. Applications of alginate-based bioinks in 3D bioprinting. *Int J Mol Sci* 2016;17:1976
 87. Huang G, Li F, Zhao X, et al. Functional and biomimetic materials for engineering of the three-dimensional cell microenvironment. *Chem Rev* 2017;117:12764-12850
 88. Handorf AM, Zhou Y, Halanski MA, Li WJ. Tissue stiffness dictates development, homeostasis, and disease progression. *Organogenesis* 2015;11:1-15
 89. Guimarães CF, Gasperini L, Marques AP, Reis RL. The stiffness of living tissues and its implications for tissue engineering. *Nat Rev Mater* 2020;5:351-370
 90. Pettikiriarachchi JTS, Parish CL, Shoichet MS, Forsythe JS, Nisbet DR. Biomaterials for brain tissue engineering. *Aust J Chem* 2010;63:1143-1154
 91. Rauti R, Renous N, Maoz BM. Mimicking the brain extracellular matrix *in vitro*: a review of current methodologies and challenges. *Israel J Chem* 2020;60:1141-1151
 92. Novak U, Kaye AH. Extracellular matrix and the brain: components and function. *J Clin Neurosci* 2000;7:280-290
 93. Bedossa P, Paradis V. Liver extracellular matrix in health and disease. *J Pathol* 2003;200:504-515
 94. Jain E, Damania A, Kumar A. Biomaterials for liver tissue engineering. *Hepatol Int* 2014;8:185-197
 95. Balestrini JL, Niklason LE. Extracellular matrix as a driver for lung regeneration. *Ann Biomed Eng* 2015;43:568-576
 96. Tebyanian H, Karami A, Nourani MR, et al. Lung tissue engineering: an update. *J Cell Physiol* 2019;234:19256-19270
 97. Lockhart M, Wirrig E, Phelps A, Wessels A. Extracellular matrix and heart development. *Birth Defects Res A Clin Mol Teratol* 2011;91:535-550
 98. Chen Q-Z, Harding SE, Ali NN, Lyon AR, Boccaccini AR. Biomaterials in cardiac tissue engineering: ten years of research survey. *Mater Sci Eng R Rep* 2008;59:1-37
 99. Hussain SH, Limthongkul B, Humphreys TR. The biomechanical properties of the skin. *Dermatol Surg* 2013;39:193-203
 100. Norouzi M, Boroujeni SM, Omidvarkordshouli N, Soleimani M. Advances in skin regeneration: application of electrospun scaffolds. *Adv Healthc Mater* 2015;4:1114-1133
 101. Stevens MM. Biomaterials for bone tissue engineering. *Mater Today* 2008;11:18-25
 102. Ho DLL, Lee S, Du J, et al. Large-scale production of wholly cellular bioinks via the optimization of human induced pluripotent stem cell aggregate culture in automated bioreactors. *Adv Healthc Mater* 2022;11:e2201138
 103. Skylar-Scott MA, Uzel SGM, Nam LL, et al. Biomanufacturing of organ-specific tissues with high cellular density and embedded vascular channels. *Sci Adv* 2019;5:eaaw2459